0.05–3 GHz VNA characterization of soil dielectric properties based on the multiline TRL calibration

2017 Meas. Sci. Technol. 28 024007

(http://iopscience.iop.org/0957-0233/28/2/024007)

OPEN ACCESS
IOP Publishing
Measurement Science and Technology
Meas. Sci. Technol. **28** (2017) 024007 (7pp)
doi:10.1088/1361-6501/28/2/024007

0.05–3 GHz VNA characterization of soil dielectric properties based on the multiline TRL calibration

Arkadiusz Lewandowski[1], Agnieszka Szypłowska[2], Marcin Kafarski[2], Andrzej Wilczek[2], Paweł Barmuta[1] and Wojciech Skierucha[2]

[1] Institute of Electronic Systems, Warsaw University of Technology, Nowowiejska 15/19, 00-665 Warsaw, Poland
[2] Institute of Agrophysics, Polish Academy of Sciences, Doświadczalna 4, 20-290 Lublin, Poland

E-mail: a.lewandowski@elka.pw.edu.pl

Received 20 July 2016, revised 12 October 2016
Accepted for publication 26 October 2016
Published 12 January 2017

Abstract

We present a methodology for characterization of soil relative dielectric permittivity in the frequency range 0.05–3 GHz. Soil samples are placed in a measurement cell constructed out of a EIA 1-5/8" coaxial transmission line, and then measured with a calibrated vector-network-analyzer. From these measurements the relative dielectric permittivity is obtained by use of a modified Boughriet algorithm. In order to calibrate the vector-network-analyzer directly at the EIA 1-5/8" coaxial-transmission-line measurement planes, we use the multiline through-reflect-line method. This method, while providing superior vector-network-analyzer calibration accuracy, is also easy to implement since it uses only transmission lines with known lengths and a single unknown highly-reflective termination. The implemented calibration method was compared to a simplified approach that uses the standard SOLT calibration in Type-N reference planes, and then accounts for the Type-N/EIA 1-5/8" adapters by removing their electrical delay. Experimental results for teflon and soil samples with different moisture content and salinity confirmed the validity of our approach.

Keywords: soil relative dielectric permittivity, vector network analyzer, multiline through-reflect-line calibration

(Some figures may appear in colour only in the online journal)

1. Introduction

Soil dielectric properties are of high interest both from the theoretical and practical point of view, especially for the purpose of soil moisture determination [1, 2]. Measurement techniques used to determine the relative dielectric permittivity of soil can be divided into time- and frequency-domain methods [3]. Time-domain methods rely on the measurement of the response to a step [4, 5] or a needle [6] pulse sent by a probe inserted into a soil sample. From the delay of this response (and its change with respect to the original pulse) the relative dielectric permittivity may be extracted. These methods are relatively simple to implement and fast. However, they enable to determine only the bulk (apparent) dielectric permittivity. Reliable measurements of complex dielectric permittivity frequency spectra using time-domain methods require high-quality equipment, careful calibrations and application of Fourier transforms [3, 7, 8]. Frequency-domain methods are based on the measurement of electrical parameters of a soil sample at a set of discrete frequencies. In the case of open-ended probes, this electrical parameter is the impedance (or equivalently the reflection coefficient); in a more general case, the soil sample is treated as a two-port network and is characterized in terms of scattering parameters [9].

Open-ended probes can be used to measure dielectric properties of fine-grained soil [10]. For the purpose of soil complex dielectric permittivity determination in a broad frequency range, coaxial transmission line cells are used [11–14] which allow to measure larger sample-volumes than the open-ended probes. Reference [14] introduces a frequency-domain approach based on wideband scattering-parameter measurements of soil samples inserted into a measurement cell constructed out of a EIA 1-5/8" coaxial transmission line. This cell is connected to a vector-network-analyzer (VNA) and from the measurement of its scattering parameters, the dielectric spectrum of the soil sample is determined. The use of a coaxial transmission lines with a large diameter allows to measure large volumes of soil which improves the measurement accuracy. However, this also introduces significant calibration problems, as there are no commercially available calibration standards in the EIA 1-5/8" coaxial transmission line. Even when using such standards, it would be difficult to shift the measurement plane from the connection plane down to the actual plane at which the soil sample begins. Thus, in [14] an approximate approach is used in which the calibration is performed with Type-N calibration standards and the cell is connected through Type-N/EIA 1-5/8" adapters. The impact of these adapters is then approximately accounted for by removing only their electrical delay.

In this work, we present a wideband scattering-parameter-based approach for the measurement of soil dielectric spectrum in which the scattering-parameters of the soil sample are determined at the reference planes at which the sample is actually inserted. To this end, a custom-designed set of calibration standards is used to implement the multiline through-reflect-line (TRL) calibration [15]. This set consists of five EIA 1-5/8" coaxial transmission lines with different lengths designed based on the methodology [16]. By defining the calibration standards in the EIA 1-5/8" coaxial-transmission-line plane, we can accurately calibrate out the Type-N/EIA 1-5/8" adapter, as opposed to the approximate approach of calibrating at the Type-N connector planes, and thus shift the measurement plane after the calibration down to the very soil sample.

2. Measurement setup

Schematic of the measurement setup is shown in figure 1(a). We performed scattering parameter measurements with the Anritsu MS4642A VNA in the frequency range 0.05 to 3 GHz. The measurement planes were set at the EIA 1-5/8" connectors which were attached to each VNA port through a cascade of a Type-N/EIA 1-5/8" adapter, a Type-N precision microwave cable, and a Type-N/3.5 mm adapter. Soil samples were inserted into a measurement cell constructed out of a 60 mm long coaxial transmission line made out of copper and then connected to measurement system through additional EIA 1-5/8" flanges. The cross-sectional dimensions of the line are specified by the EIA RS-225 standard: the inner diameter of the outer conductor is 38.8 mm $\pm$ 0.075 mm while the outer diameter of the inner conductor is 16.9 mm $\pm$ 0.050 mm. The diameters of the inner and outer conductors were specifically chosen in order to measure large sample volume, which is important for inhomogeneous materials, such as soil. These dimensions were analogous to the setup used for soil samples measurements in [14].

Prior to the characterization of the measurement cell with soil samples, the VNA was calibrated with the multiline TRL method [15] which is commonly considered as the most accurate technique for the vector-network-analyzer (VNA) calibration. This method uses a set of transmission lines with different lengths and the same but otherwise unknown propagation constant, a reflect standard which is assumed to be identical on both VNA ports but otherwise unknown, and a thru connection. All of the unknown parameters of the calibration standards, that is, the propagation constant of the lines and the reflection coefficient of the reflect standard are then determined along with the VNA calibration coefficients [15].

In order to implement the multiline TRL method in our measurement environment, we designed a set of five EIA 1-5/8" coaxial transmission lines by use of the method [16]. A picture of this set is shown in figure 1(b): the longest line is 500 mm while the shortest one is 60 mm. The method [16] allows to choose the line lengths so as to obtain an accurate calibration in a given measurement bandwidth (which is 0.05 to 3 GHz in our case). In order to obtain an accurate calibration at lower frequencies, the longest line should be in general made as long as possible. We limited the length of this line to 500 mm long for practical reasons, since connecting a longer line would be very difficult.

The calibration lines were manufactured out of copper and have the same diameters as the measurement cell. They were connected to the VNA measurement ports through additional EIA 1-5/8" flanges. As a reflect standard [15], we used an open circuit constructed by connecting to the EIA 1-5/8" flange a shielded section of the outer conductor. We implemented the multiline TRL calibration procedure [15] in the MATLAB environment [17]. In the VNA calibration and error correction we used the model proposed in [18].

It is important to note that the use of calibration standards implemented at the EIA 1-5/8" measurement plane has two significant advantages. First, by defining the calibration standards in this plane, we can accurately calibrate out the Type-N/EIA 1-5/8" adapter. Secondly, the multiline TRL calibration allows us to calibrate out also the discontinuity occurring at the connection plane (due to the center-conductor support element). Indeed, since the transmission lines are defined as reflection-less (with respect to their characteristic impedance) and the connection-plane discontinuity is identical for all connected elements, its electrical parameters are lumped into the VNA calibration coefficients. Thus, we can obtain scattering-parameter measurement of the measurement cell itself.

3. Modeling and extraction

We model the scattering-parameter measurement of the cell based on figure 2. The measurement cell can be described as a cascade connection of transmission lines with different dielectrics: sections $A1$ and $A2$ correspond to the short air

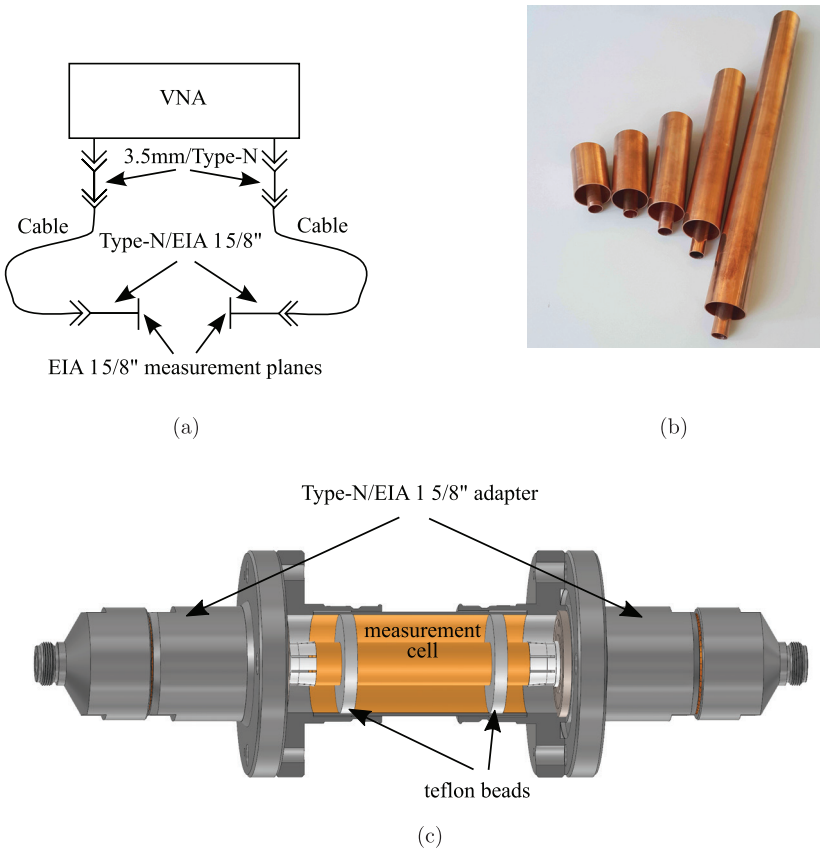

Figure 1. Measurement setup: (a) schematic, (b) EIA 1-5/8" coaxial transmission lines used as calibration standards, (c) three-dimensional view of the measurement cell connected to the Type-N/EIA 1-5/8" adapters.

gaps, sections $T1$ and $T2$ describe the teflon beads supporting the sample and the center conductor, while section M corresponds to the line filled with the material under test (MUT).

In order to model the scattering parameters of the cell, we use the transmission-matrix description. For a two-port network, the scattering matrix $\mathbf{S}$ and transmission matrix $\mathbf{T}$ are defined as [19]:

$$\begin{bmatrix} b_1 \\ b_2 \end{bmatrix} = \mathbf{S} \begin{bmatrix} a_1 \\ a_2 \end{bmatrix}, \text{ and } \begin{bmatrix} b_1 \\ a_1 \end{bmatrix} = \mathbf{T} \begin{bmatrix} a_2 \\ b_2 \end{bmatrix} \tag{1}$$

where

$$\mathbf{S} = \begin{bmatrix} S_{11} & S_{12} \\ S_{21} & S_{22} \end{bmatrix}, \text{ and } \mathbf{T} = \frac{1}{S_{21}} \begin{bmatrix} -\det \mathbf{S} & S_{11} \\ -S_{22} & 1 \end{bmatrix}. \tag{2}$$

It can be easily shown that for a cascade connection of two-port networks with transmission matrices $\mathbf{T}_i$, for $i = 1, \ldots, N$, referenced to the same impedance Z_{ref}, the overall transmission matrix is given by a product $\mathbf{T}_1\mathbf{T}_2 \cdot \ldots \cdot \mathbf{T}_N$ [19]. Thus, for the model given in figure 2, we can write the measured transmission matrix as:

$$\mathbf{T}_{\text{cell}} = \mathbf{T}_{\text{A1}}\mathbf{T}_{\text{T1}}\mathbf{T}_{\text{M}}\mathbf{T}_{\text{T2}}\mathbf{T}_{\text{A2}}. \tag{3}$$

Since we know the lengths of the the teflon and air sections, we can determine their transmission matrices $\mathbf{T}_{\text{A1}}$, $\mathbf{T}_{\text{A2}}$, $\mathbf{T}_{\text{T1}}$, and $\mathbf{T}_{\text{T2}}$, and from the measured transmission matrix of the cell determine the transmission parameters of the sample itself as:

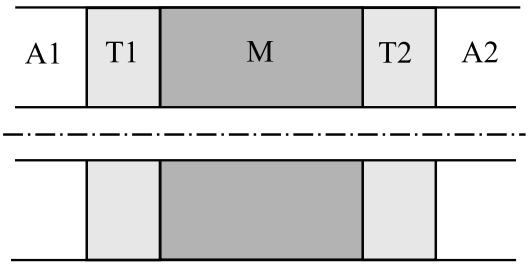

Figure 2. Cross-section of the measurement cell.

$$\mathbf{T}_{\text{M}} = (\mathbf{T}_{\text{A1}}\mathbf{T}_{\text{T1}})^{-1}\mathbf{T}_{\text{cell}}(\mathbf{T}_{\text{T2}}\mathbf{T}_{\text{A2}})^{-1}. \tag{4}$$

In order to evaluate (4), we need to write transmission parameters of each transmission-line section in figure 2 with respect to the same reference impedance Z_{ref}. Expressing first these parameters with respect to the line characteristic impedance Z_0 (which is different for each section) we obtain [20]:

$$\mathbf{T}_l^0 = \begin{bmatrix} \mathrm{e}^{-\gamma l} & 0 \\ 0 & \mathrm{e}^{\gamma l} \end{bmatrix} \tag{5}$$

where γ is the complex propagation constant and l is the length of the line section. Assuming a non-magnetic dielectric with a relative dielectric permittivity ε_{r} and neglecting conductor loss[3], we can write the propagation constant $\gamma = \mathrm{j}\omega/c\sqrt{\varepsilon_{\text{r}}}$

[3] We assume that the conductor loss in the coaxial-line walls is much smaller than the dielectric loss of the soil sample.

Table 1. Particle-size distribution (PSD) of the soil material.

Particle sizes (μm)	0.01–2	2–20	20–50	50–100	100–250	250–500	500–1000	1000–2000
PSD (%)	0.50	4.01	5.64	2.49	11.06	49.29	26.63	0.38

and the characteristic impedance $Z_0 = \eta/\sqrt{\varepsilon_r}$, where c is the speed of light in vacuum and η is the characteristic impedance of the coaxial transmission line with vacuum-dielectric[4]. By comparing (5) with (2), we note that $S_{11} = S_{22} = 0$, which is a direct consequence of the fact that a line is impedance-matched to its characteristic impedance Z_0. Rewriting (5) with respect to an arbitrary reference impedance Z_{ref} we obtain [20]:

$$\mathbf{T}_l = \frac{e^{\gamma l}}{1-\Gamma_l^2}\begin{bmatrix} e^{-2\gamma l}-\Gamma_l^2 & (1-e^{-2\gamma l})\Gamma_l \\ -(1-e^{-2\gamma l})\Gamma_l & 1-e^{-2\gamma l}\Gamma_l^2 \end{bmatrix} \tag{6}$$

where $\Gamma_l = \frac{Z_0 - Z_{\text{ref}}}{Z_0 + Z_{\text{ref}}}$.

Reference impedance Z_{ref} can be chosen arbitrarily. However, it is convenient to set Z_{ref} to the characteristic impedance $Z_{0A} = \eta/\sqrt{\varepsilon_{rA}}$ of the air-filled sections, where ε_{rA} is the dielectric permittivity of air. This is due to the fact that a VNA calibrated with the multiline TRL calibration measures scattering-parameters with respect to the characteristic impedance of the transmission lines used in the calibration [15, 20]. In this work we use air-filled coaxial transmission lines so the reference impedance of the multiline TRL calibration is precisely Z_{0A}.

Having determined the transmission matrix of the MUT from (4), we convert it to the scattering-parameter representation by inverting (2). We then apply the extraction algorithm described in appendix to obtain the relative dielectric permittivity of the MUT.

4. Materials

In order to verify our system, we measured a 20.6 mm thick teflon sample inserted into the measurement cell. After that, several soil samples of various water content and salinity were examined. All of the soil samples were prepared based on a sandy soil material (texture: sand 89.9%, silt 9.6%, clay 0.5%) by adding a predefined amount of moistening liquid and mixing. The particle-size distribution was measured by the laser diffraction method according to the procedure described in [21] and was presented in table 1. The values of water content θ_M calculated on a dry mass basis, mass m, volume V, volumetric water content θ_V, and bulk density d were listed in table 2.

Soil material of three various initial salinities was used. The initial salinity was characterized on the basis of electrical conductivity σ_e of 1:5 (w/v) soil-distilled water extracts [22], and the values were presented in table 2. Soil samples with the designator A were obtained by wetting the least saline soil material with distilled water to achieve three levels of water content up to saturation. Samples with the designator B were obtained from the more saline soil material as A samples. They were wetted up to the same target moisture of $\theta_M = 0.10$ g g^{-1} (on a dry mass basis) with either distilled water (samples $B1$ and $B2$) or a KCl solution (sample $B3$) of electrical conductivity 2 S m^{-1}.

[4] These expressions are valid only for TEM lines such as the coaxial transmission line discussed in this paper; for waveguides with non-zero cutoff frequency one would have to additionally include the frequency dependence of the group velocity.

Table 2. Parameters of the soil samples.

Sample	σ_e (mS m^{-1})	θ_M (g g^{-1})	m (g)	V (cm^3)	θ_V (%)	d (g cm^{-3})
$A0$	3.21	air-dry	80.98	44.26	air-dry	1.83
$A1$	3.21	0.05	77.60	45.62	8.1	1.70
$A2$	3.21	0.10	90.86	45.34	18.2	2.00
$A3$	3.21	0.14	96.16	45.31	26.1	2.12
$B1$	18.72	0.10	95.06	47.22	18.3	2.01
$B2$	36.38	0.10	93.70	47.37	18.0	1.98
$B3$	36.38	0.10	94.06	47.04	18.2	2.00

After preparation, each soil sample was placed between the inner and outer conductor of the 60 mm long measurement cell, supported by two 4 mm thick teflon beads. The precise positions of the supporting beads for each tested sample were measured and accounted for in the permittivity extraction algorithm. The dielectric measurements of the samples were performed at room temperature 22 ± 1 °C.

5. Results and discussion

In figure 3 we present results for the teflon sample used as a reference material. These results were obtained with the use of the VNA error-correction procedure based on the multiline TRL calibration (see section 2) and compared with a simplified error correction method proposed in [14]. This simplified procedure uses a classical two-port short-open-load-thru (SOLT) calibration procedure to calibrate the VNA in the Type-N reference planes and then corrects for the impact of Type-N/EIA 1-5/8" adapters by removing only their electrical length.

We see that the real part of the dielectric permittivity of teflon sample obtained with our procedure agrees very well with the literature: in the frequency range 0.05–3 GHz we obtained flat spectrum with $\varepsilon' = 2.07 \pm 0.02$ which differs from $\varepsilon' = 2.035 \pm 0.005$ reported in [9] by around 1.7%. We also see that the imaginary part ε'' is close the noise floor of our measurement system.

We further see the the spectrum obtained with the simplified error-correction procedure gives for small frequencies values of ε' by almost 10% smaller than expected for teflon and that it also overestimates the loss. This can be easily justified with the fact that by correcting only for the electrical length of the adapters, we lump their loss into the consecutive MUT measurements.

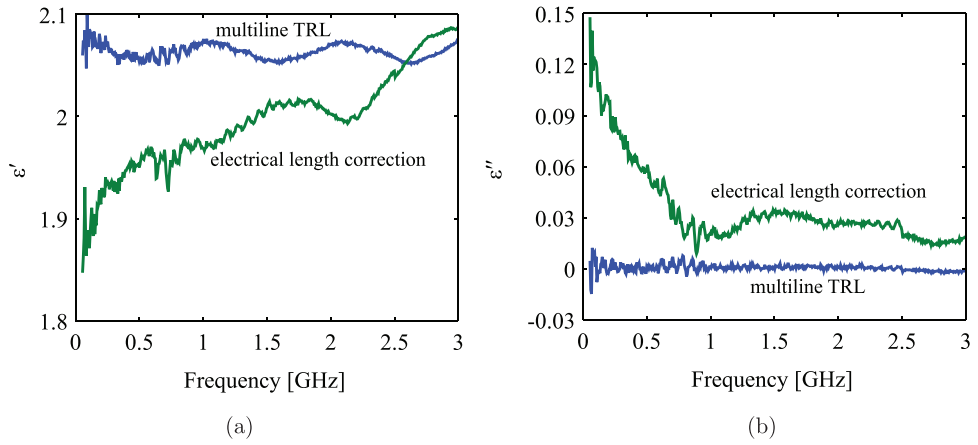

Figure 3. Measurement results for a 20.6 mm thick teflon sample obtained with a VNA error-correction based on the multiline TRL calibration (solid blue) and with a simplified error correction taking into account only the electrical length of the Type-N/EIA 1-5/8" adapters: (a) ε_r' and (b) ε_r'' .

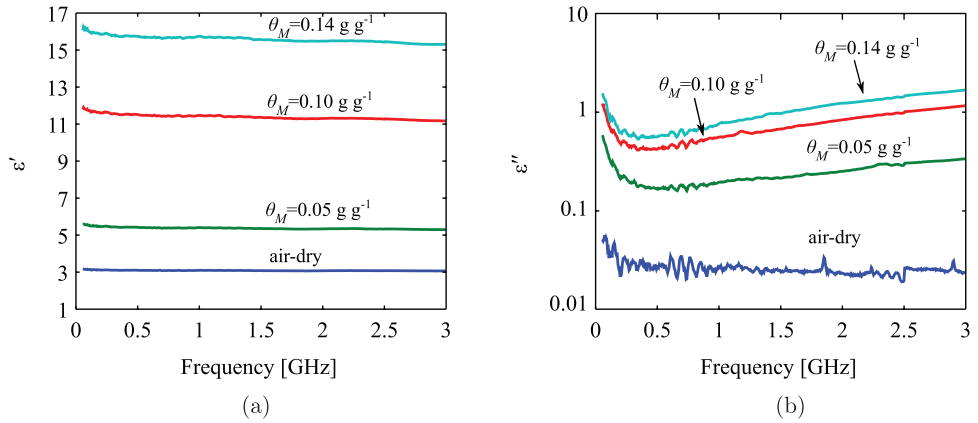

Figure 4. Measurement results for non-saline soil samples with different moisture content: (a) ε_r' and (b) ε_r''.

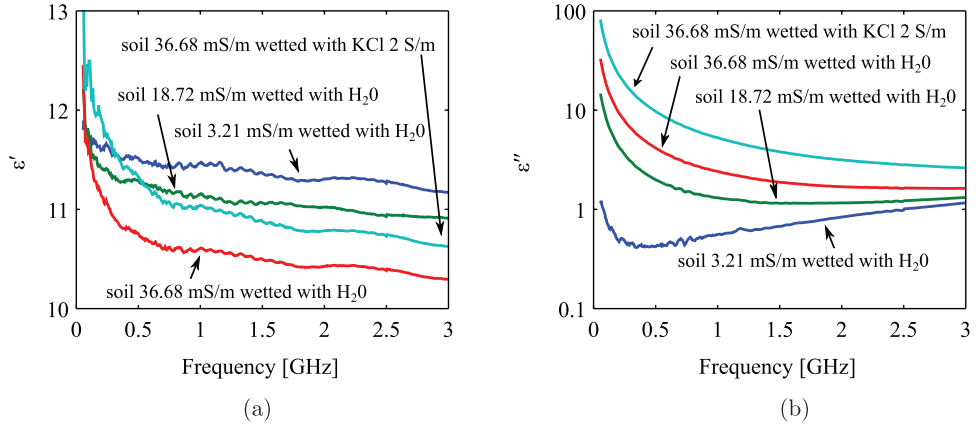

Figure 5. Measurement results for different saline-soil samples and for a reference non-saline soil sample: (a) ε_r' and (b) ε_r''. All presented samples were wetted to achieve the target moisture $\theta_M = 0.10$ g g^{-1}.

In figure 4 we present dielectric spectra for non-saline soil samples. We see that the real part ε' of the dielectric permittivity (see figure 4(a)) increased with the moisture content of the samples and varied from about 3 for the air-dry sample to a little over 16 for the saturated one. As expected for soil with a small clay content, the permittivity values did not decrease much with the increase of frequency.

Although all of the presented saline samples were wetted to achieve the same target moisture θ_M, the real part of dielectric permittivity varied among the samples (see figure 5(a)). It was caused by slight differences in bulk density (see table 2). Also, evaporation during sample preparation could have influenced the final water content.

The imaginary part ε'' of dielectric permittivity of the air-dry sample was under 0.1 in the entire frequency range with

relatively small scatter (see figure 4(b)). The impact of bulk electrical conductivity on the imaginary part of dielectric permittivity was observed even for non-saline wet samples at frequencies below 0.5 GHz. For the saline-soil samples (see figure 5(b)), the imaginary part ε'' of the dielectric permittivity rose significantly at low frequencies. For the most saline *B*3 sample, electrical conductivity dominated the ε'' spectrum in the entire applied frequency range.

The dielectric permittivity spectra of the samples of various moisture content obtained from the same non-saline soil as in the present study was examined in the 0.1–1.2 GHz frequency range in [8]. The results obtained in the present work agreed with the previous findings.

6. Conclusions

In this work, we presented a technique for wideband 0.05–3 GHz characterization of soil dielectric spectra by use of vector-network-analyzer (VNA) scattering-parameter measurements. Our technique is based on VNA measurement of soil samples inserted into a EIA 1-5/8" coaxial-transmission-line cell. Before the measurements, the VNA is calibrated with the multiline through-reflect-line (TRL) method [15] with a custom-designed [16] set of calibration standards based on the EIA 1-5/8" coaxial-transmission-line. The use of calibration standards defined in the same waveguiding structure as the measurement cell makes it possible to remove the systematic errors due to the cell connectors, and thus set the measurement planes at the soil sample itself. Experimental results for teflon and soil samples with different water content and salinity verified the validity of our approach.

Acknowledgments

Arkadiusz Lewandowski has been supported by the Polish National Science Center in the framework of the project no. 2011/03/D/ST7/01731.

Appendix

Below we briefly summarize the extraction algorithm. From transmission parameters of the MUT we obtain scattering parameters by inverting (2) which yields the following model of the MUT measurement:

$$\mathbf{S}_{\mathrm{M}} = \frac{1}{1-\Gamma_{\mathrm{M}}^2 \mathrm{e}^{-2\gamma_{\mathrm{M}} l}} \begin{bmatrix} (1-\mathrm{e}^{-2\gamma_{\mathrm{M}} l})\Gamma_{\mathrm{M}} & \mathrm{e}^{-\gamma_{\mathrm{M}} l}(1-\Gamma_{\mathrm{M}}^2) \\ \mathrm{e}^{-\gamma_{\mathrm{M}} l}(1-\Gamma_{\mathrm{M}}^2) & (1-\mathrm{e}^{-2\gamma_{\mathrm{M}} l})\Gamma_{\mathrm{M}} \end{bmatrix} \quad \text{(A.1)}$$

where for Z_{ref} set to $Z_{0\mathrm{A}} = \eta/\sqrt{\varepsilon_{\mathrm{rA}}}$ we further have:

$$\Gamma_{\mathrm{M}} = \frac{1-\sqrt{\frac{\varepsilon_{\mathrm{rM}}}{\varepsilon_{\mathrm{rA}}}}}{1+\sqrt{\frac{\varepsilon_{\mathrm{rM}}}{\varepsilon_{\mathrm{rA}}}}}, \text{ and } \gamma_{\mathrm{M}} = \mathrm{j}\frac{\omega}{c}\sqrt{\varepsilon_{\mathrm{rM}}}. \quad \text{(A.2)}$$

The problem now is to determine ε_{rM} from the actual scattering parameters of the MUT obtained by applying the correction equation (4) to the measured transmission matrix $\mathbf{T}_{\mathrm{cell}}$ of the cell. From the classical Nicholson–Ross–Weir equations [9, 23] we obtain the estimate of Γ_{M} as:

$$\hat{\Gamma}_{\mathrm{M}} = K \pm \sqrt{K^2-1}, \text{ where } K = \frac{S_{11}^2 - S_{21}^2 + 1}{2S_{11}}. \quad \text{(A.3)}$$

In order to choose the proper sign in (A.3), we enforce $|\hat{\Gamma}_{\mathrm{M}}| \leqslant 1$. From this estimate we can then determine the estimate of the term $T = \mathrm{e}^{-\gamma_{\mathrm{M}} l}$ as:

$$\hat{T} = \frac{S_{11} + S_{21} - \hat{\Gamma}_{\mathrm{M}}}{1-(S_{11}+S_{21})\hat{\Gamma}_{\mathrm{M}}}. \quad \text{(A.4)}$$

Consecutively, we obtain the estimate of γ_{M} as:

$$\hat{\gamma}_{\mathrm{M}} = -\frac{\ln \hat{T}}{l}. \quad \text{(A.5)}$$

In order to select the proper root of the natural logarithm, we enforce the continuous change of $\hat{\gamma}_{\mathrm{M}}$ as a function of frequency. Eventually, we determine the relative dielectric permittivity of the MUT as:

$$\hat{\varepsilon}_{\mathrm{rM}} = -\frac{c\hat{\gamma}_{\mathrm{M}}^2}{\omega}. \quad \text{(A.6)}$$

As we can see, the choice of Z_{ref} does not affect the extraction algorithm. Indeed, it only changes the reflection coefficient Γ_{M}, however, this term is not further decomposed in order to solve for $\varepsilon_{\mathrm{rM}}$.

References

[1] Robinson D A, Campbell C S, Hopmans J W, Hornbuckle B K, Jones S B, Knight R, Ogden F, Selker J and Wendroth O 2008 Soil moisture measurement for ecological and hydrological watershed-scale observatories: a review *Vadose Zone J.* **7** 358–89

[2] Bittelli M 2011 Measuring soil water content: a review *HortTechnology* **21** 293–300

[3] Kaatze U and Huebner C 2010 Electromagnetic techniques for moisture content determination of materials *Meas. Sci. Technol.* **21** 082001

[4] Topp G C, Davis J L and Annan A P 1980 Electromagnetic determination of soil water content: measurement in coaxial transmission lines *Water Resour. Res.* **16** 574–82

[5] Noborio K 2001 Measurement of soil water content and electrical conductivity by time domain reflectometry: a review *Comput. Electron. Agric.* **31** 213–37

[6] Skierucha W, Wilczek A, Szypłowska A, Sławiński C and Lamorski K 2012 A tdr-based soil moisture monitoring system with simultaneous measurement of soil temperature and electrical conductivity *Sensors* **12** 13545–66

[7] Kaatze U and Feldman Y 2006 Broadband dielectric spectrometry of liquids and biosystems *Meas. Sci. Technol.* **17** R17–35

[8] Szypłowska A, Wilczek A, Kafarski M and Skierucha W 2016 Soil complex dielectric permittivity spectra determination using electrical signal reflections in probes of various lengths *Vadose Zone J.* **15**

[9] Baker-Jarvis J 1990 TN 1341: transmission/reflection and short-circuit line permittivity measurements *Technical Report* NIST

[10] Wagner N, Schwing M and Scheuermann A 2014 Numerical 3-d fem and experimental analysis of the open-ended coaxial line technique for microwave dielectric spectroscopy on soil *IEEE Trans. Geosci. Remote Sens.* **52** 880–93
[11] Wagner N, Emmerich K, Bonitz F and Kupfer K 2011 Experimental investigations on the frequency- and temperature-dependent dielectric material properties of soil *IEEE Trans. Geosci. Remote Sens.* **49** 2518–30
[12] Bobrov P P, Repin A V and Rodionova O V 2015 Wideband frequency domain method of soil dielectric property measurements *IEEE Trans. Geosci. Remote Sens.* **53** 2366–72
[13] Ba D and Sabouroux P 2010 Epsimu, a toolkit for permittivity and permeability measurement in microwave domain at real time of all materials: applications to solid and semisolid materials *Microw. Opt. Technol. Lett.* **52** 2643–8
[14] Lauer K, Wagner N and Felix-Henningsen P 2012 A new technique for measuring broadband dielectric spectra of undisturbed soil samples *Eur. J. Soil Sci.* **63** 224–38
[15] Marks R B 1991 A multiline method of network analyzer calibration *IEEE Trans. Microw. Theory Technol.* **39** 1205–15
[16] Lewandowski A, Wiatr W, Opalski L J and Biedrzycki R 2015 Accuracy and bandwidth optimization of the over-determined offset-short reflectometer calibration *IEEE Trans. Microw. Theory Technol.* **63** 1076–1089
[17] MathWorks 2014 *MATLAB R2014a* www.mathworks.com/products/matlab/
[18] Marks R B 1997 Formulations of the basic vector network analyzer error model including switch-terms *50th ARFTG Conf. Digest (Portland, OR, December 1997)* vol 32 pp 115–26
[19] Kerns D M and Beatty R W 1967 *Basic Theory of Waveguide Junctions and Introductory Microwave Network Analysis* (Oxford: Pergamon)
[20] Marks R B and Williams D F 1992 A general waveguide circuit theory *Natl Inst. Stand. Technol. J. Res.* **97** 533–62
[21] Bieganowski A, Chojecki T, Ryżak M, Sochan A and Lamorski K 2013 Methodological aspects of fractal dimension estimation on the basis of psd *Vadose Zone J.* **12**
[22] Rhoades J D, Chanduvi F and Lesch S 1999 *Soil Salinity Assessment, Interpretation of Electrical Conductivity Measurements (Food and Agriculture Organization of the United Nations)*
[23] Boughriet A-H, Legrand C and Chapoton A 1997 Noniterative stable transmission/reflection method for low-loss material complex permittivity determination *IEEE Trans. Microw. Theory Technol.* **45** 52–7